Regulation of chromenylium fluorophore with a built-in recognition site for the detection of sulfite

Anqi Hou,[a,b] Yuanyuan Wu,[a,b] Yumeng Liu,[a,b] Chang Liu*[a,b], Huirong Yao*[a,b] and Xianshun Zeng*[a,b]

[a] *Tianjin Key Laboratory for Photoelectric Materials and Devices, School of Materials Science & Engineering, Tianjin University of Technology, Tianjin 300384, China.*

[b] *Key Laboratory of Display Materials & Photoelectric Devices, Ministry of Education, School of Materials Science & Engineering, Tianjin University of Technology, Tianjin 300384, China.*

**Corresponding author: Tel: (+86)22-60216748;*

E-mail: xshzeng@tjut.edu.cn；liuchang1014@126.com

1. Materials and methods

We purchased 2-[4-(diethylamino)-2-hydroxybenzoyl] benzoic acid, 7,8-dihydro-6H-quinolin-5-one, methyl alcohol, methyl iodide and sodium sulfite (Na_2SO_3) from Aladdin (Shanghai, China). All chemicals and solvents used for synthesis were purchased from commercial suppliers and applied directly in the experiment without further purification 3-(4,5-dimethylthiazol-2-yl)-2,5-diphenyltetrazolium bromide (MTT) purchased from Beyotime Institute of Biotechnology. ^1H NMR and ^{13}C NMR were measured on a Bruker AVANCE III HD 400MHz spectrometer. Chemical shifts (d values) were reported in ppm down field from internal Me4Si. High resolution mass spectra (HRMS) were acquired on an Agilent 6510 Q-TOF LC/MS instrument (Agilent Technologies, Palo Alto, CA) equipped with an electrospray ionization (ESI) source. Melting points were recorded on a melting point apparatus (RY-2, Tianjin, China). UV-vis absorption spectra were obtained with UV-2550 (Shimadzu, Japan) spectrophotometer. A Hitachi F-4600 spectrophotometer (Tokyo, Japan) was used for fluorescence measurements with a 700 V PMT voltage. The pH values were reported by a Mettler Toledo Seven Excellence PH meter (Shanghai, China). The absorbance for MTT analysis was recorded on a microplate reader (PL-9602). The confocal microscopy imaging was used Olympus FV1000-IX81 inverted fluorescence microscope. Image processing was analyzed with Olympus software (FV1000-ASW).

2. General procedure for fluorescence detection

The stock solution of **DMCQ** (5.0 mM) and sulfite (1 mM) were prepared by dissolving **DMCQ** and Na_2SO_3 in dimethyl sulfoxide (DMSO) and ultrapure water, respectively. Meanwhile, we obtained different concentrations of working solutions by diluting the corresponding stock solution. Other kinds of stock solutions including thiols, anions, cations, and amino acids were gained in ultrapure water. For the fluorescence scanning, the excitation and emission wavelength were set at 520 nm. The voltage of the photomultiplier was set at 700 V and the excitation and emission slit widths were 10 nm × 10 nm. Every test was replicated three times.

3. Measurement of fluorescence quantum yield

Fluorescence quantum yield (Φ) was determined using rhodamine B (Φ_s=0.71, in ethanol) as the fluorescence standard. The quantum yield was calculated using the following equation[S1]:

$$\Phi = \Phi_s (F/F_s)(A/A_s)(\eta^2/{\eta_s}^2)$$

Where Φ and Φ_s represented the fluorescence quantum yields of the target substance and rhodamine B, respectively. F and F_s indicated the peak fluorescence emission of the target substance and rhodamine B, respectively. A and A_s denoted the maximum absorbance values of the target substance and rhodamine B, respectively. η and η_s were the refractive index of the solvent of the target substance and rhodamine B.

4. Determination of detection limit (LOD)

The standard deviation of the blank was determined by 11 measurements of the fluorescence emission spectra of the probe (5 μM). The linear relationship between the concentration of SO_2 and the fluorescence intensity at 761 nm was determined by fitting a concentration-dependent fluorescence curve. The limit of detection (LOD) was calculated using the following equation[S2]:

$$LOD = 3\sigma/k$$

Where σ was the standard deviation of the blank sample, k was the slope of the linear regression formula.

5. Measurement of the fluorescence turn-on constant ($K_{turn\text{-}on}$)[S3]

$K_{turn\text{-}on}$ was determined by fluorescence spectroscopy. Fluorescence spectra of the probe (5 μM) were measured in H2O-EtOH = 3:1 (v/v) upon addition of different amounts of Na_2SO_3. Excitation was performed at 520 nm. The fluorescent intensity data were fit to the following equation to calculate $K_{turn\text{-}on}$:

The equation used for $K_{turn\text{-}on}$ fitting can be derived as follows :

$$F = (\alpha_1 K_{turn\text{-}on} + \alpha_2[M])[L]total/ ([M]+ K_{turn\text{-}on})$$

$$L + M \rightleftharpoons L\cdot M$$

$$K_{turn\text{-}on} = [L]\,[M]/[\,L\cdot M]$$

$$\because [L]total = [L]+ [L\cdot M]$$

$$[L] = K_{turn\text{-}on}[L]total/(K_{turn\text{-}on}+[M])$$

$$[L\cdot M] = [L][\,M]/K_{turn\text{-}on}$$

$$\therefore [L]total = K_{turn\text{-}on}[L]total/(K_{turn\text{-}on}+[M]) + [L][\,M]/K_{turn\text{-}on}$$

The fluorescence intensity will have a linear relationship with each species of [L]total without considering interchomophoric interactions. The equation for fluorescent intensity would be:

$$F_{\text{total}} = \alpha_1[L]+ \alpha_2[L\cdot M] = (\alpha_1 K_{turn\text{-}on} + \alpha_2[M])[L]total/ ([M]+ K_{turn\text{-}on})$$

where α_1, α_2 represent a proportionality parameter of fluorescent species. Finally, Origin software was used to fit above nonlinear plot to give the $K_{turn\text{-}on}$ value.

6. Fluorescence imaging in living cells

The 293 cells were seeded and cultured in DMEM supplied with 1% antibiotics (100 U/mL penicillin and 100 μg/mL streptomycin) and 10% fetal bovine serum (FBS) in an atmosphere of 37 °C and 5% CO_2. For the control group, cells were incubated directly with **DMCQ** (3 μM) for 30 min at 37 °C. For the imaging of exogenous of sulfite, the cells were added with different concentrations of Na_2SO_3 (0, 10, 20 and 30 μM) for 30 min and then **DMCQ** (3 μM) for 30 min at 37 °C. For the imaging of endogenous of sulfite, cells were initially added with the SO_3^{2-} donor GSH (600 μM) and $Na_2S_2O_3$ (300 μM) for 30 min, then incubated with **DMCQ** (3 μM) for 30 min at 37 °C. In each group, all the cells were washed with PBS buffer solution (pH=7.4) three times, and the fluorescence image was performed by confocal fluorescence microscopy.

7. Sugar and water sample preparation

7.5 g of white sugar and crystal sugar was added into 30 mL of ultrapure water, respectively. Meanwhile Mineral water and tap water were also collected and used directly to detect the source of sulfur dioxide derivatives.

8. Abbreviations

DCM- Dichloromethane, DMSO- Dimethylsulfoxide, EtOH- Ethanol, MeCN- Acetonitrile, MeOH- Methanol.

9. Experiment data

Table S1 Photophysical properties of **DMCQ** in different solvents

Solvents	λ_{max} (nm)	ε ($M^{-1}cm^{-1}$)	PL_{max} (nm)	Φ	Stokes shift (nm)
H_2O	555	9600	590	0.004	35
EtOH	557	10900	611	0.028	54
MeOH	555	9300	607	0.020	52
DCM	559	12300	603	0.003	44
DMSO	565	6700	609	0.010	44
CH_3CN	554	10100	595	0.006	41

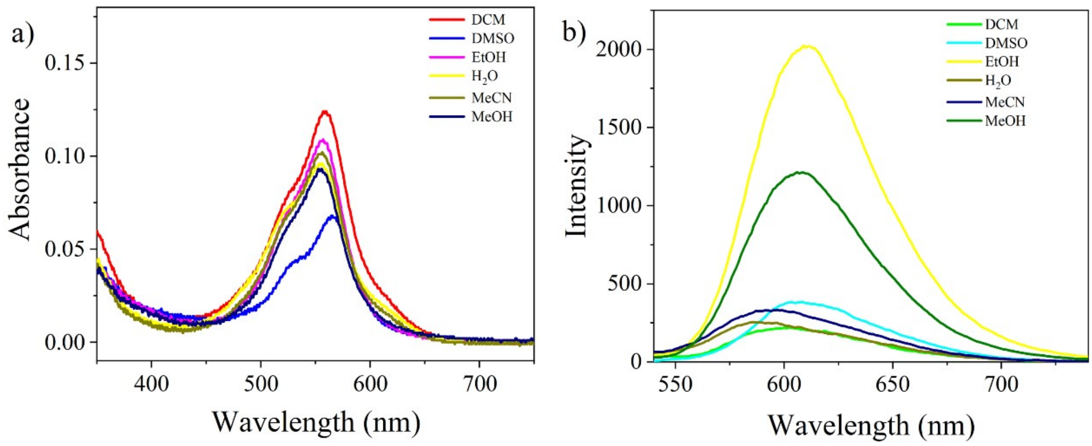

Fig S1. a) UV/vis absorption (10 μM) and b) fluorescence emission (5 μM) spectra of the probe in different solvents. λ_{ex} = 520 nm, slit = 10 nm.

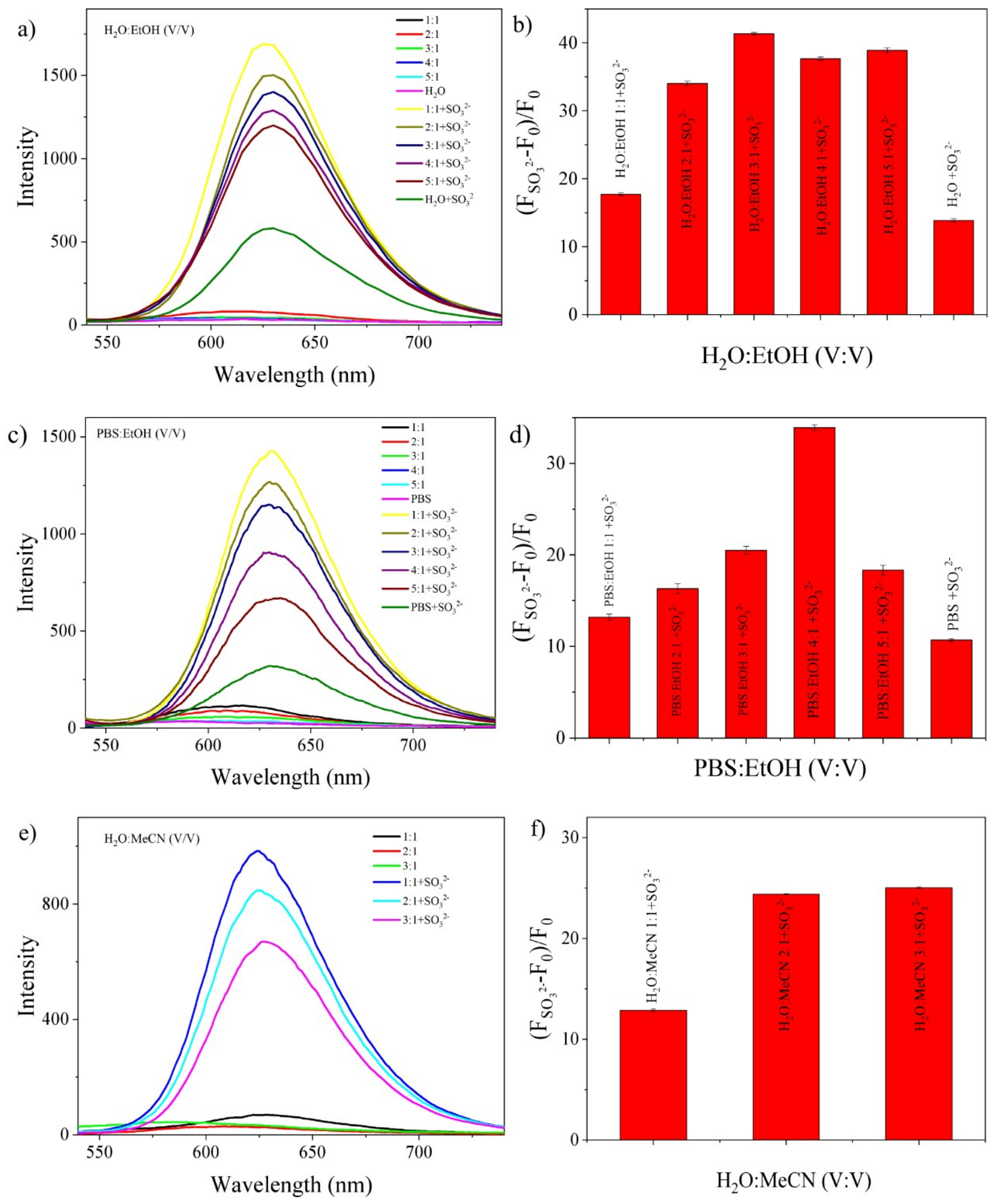

Fig. S2 Fluorescence intensity of **DMCQ** (5 μM) at 630 nm upon the addition of SO_3^{2-} (20 equiv.) in different systems. λ_{ex} = 520 nm, slit = 10 nm.

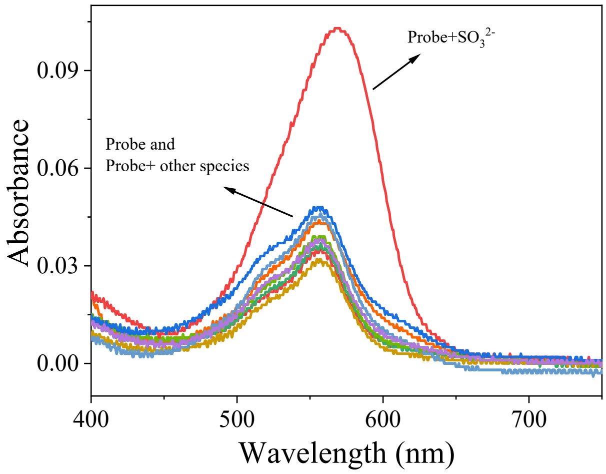

Fig. S3 Absorption spectra of **DMCQ** (10 μM) in H_2O-EtOH = 3:1 (v/v) in the presence of 20 equiv. various related analytes.

Fig. S4 Color changes of **DMCQ** (5 μM) in the presence of 20 equiv. of various analytes in H_2O/EtOH = 3:1 (v/v).

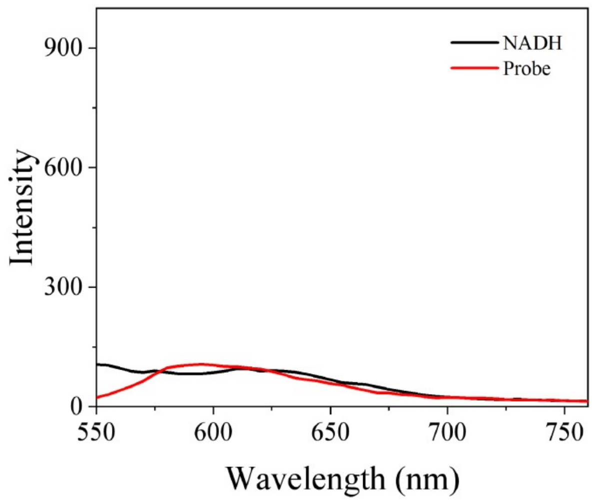

Fig. S5 Fluorescence spectra of **DMCQ** (5 μM) in H_2O-EtOH = 3:1 (v/v) upon the addition of 20 equiv. NADH. λ_{ex} = 520 nm, slit = 10 nm.

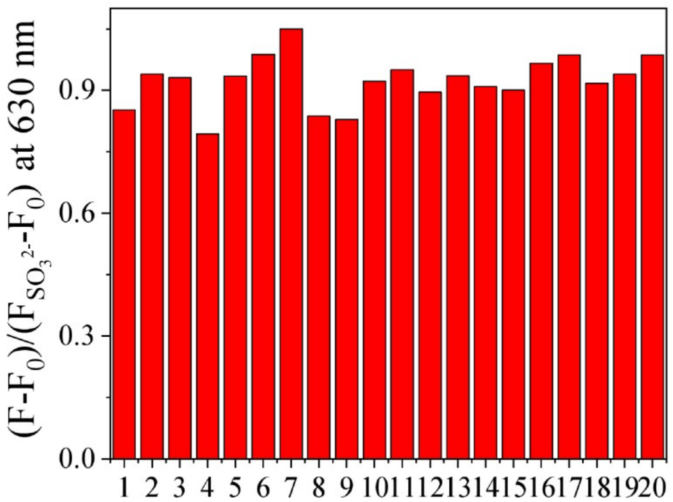

Fig. S6 Fluorescence intensity of the probe (5 μM) in H_2O/EtOH (3/1, v/v) solution with the addition of various analytes (50 μM). 1: probe + Mg^{2+} + SO_3^{2-}; 2: probe + Ca^{2+} + SO_3^{2-}, 3: probe+ Cu^{2+} + SO_3^{2-}, 4: probe + Zn^{2+}+ SO_3^{2-}, 5: probe + Na^+ + SO_3^{2-}, 6: probe + NADH + SO_3^{2-}, 7: probe + Cl^- + SO_3^{2-}, 8: probe + Br^- + SO_3^{2-}, 9: probe + F^- + SO_3^{2-}, 10: probe + I^- + SO_3^{2-}, 11: probe + HCO_3^- + SO_3^{2-}, 12: probe + HSO_4^- + $S_2O_3^{2-}$, 13: probe + OAC^- + SO_3^{2-}, 14: probe + SO_4^{2-} + SO_3^{2-}, 15: probe + GSH + SO_3^{2-}, 16: probe + Hcy + SO_3^{2-}, 17: probe + Cys + SO_3^{2-}, 18: probe +DTT + SO_3^{2-}, 19: probe + HS^- + SO_3^{2-}, 20: probe + SO_3^{2-}; λ_{ex} = 520 nm, slit = 10 nm.

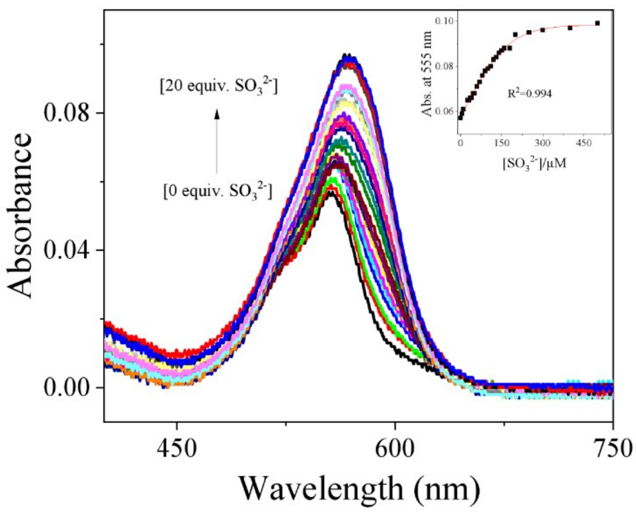

Fig. S7 UV-vis spectra of **DMCQ** (10 μM) in the presence of different concentrations of SO_3^{2-} in H_2O/EtOH = 3:1 (v/v). Inset: Linear relationship between the absorbance at 555 nm and SO_3^{2-} concentrations.

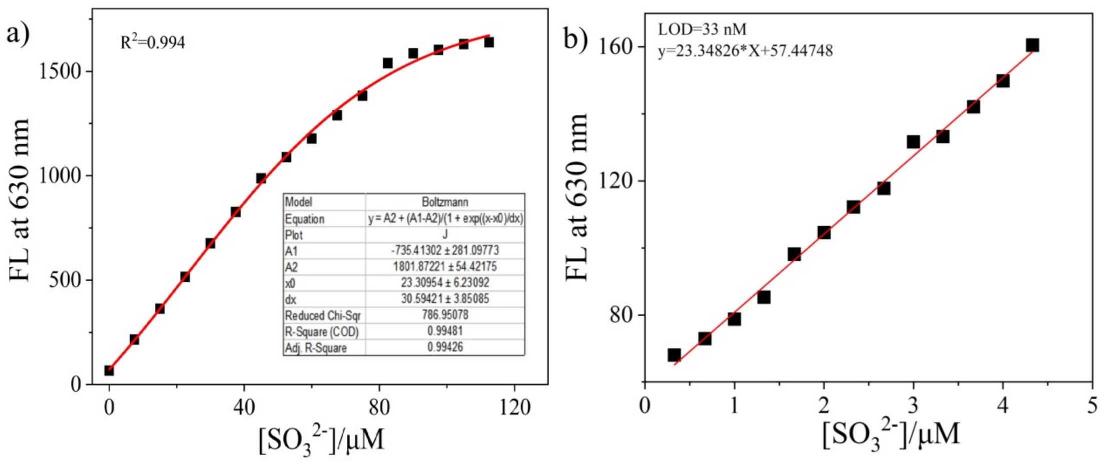

Fig. S8 The fluorescence at 630 nm of **DMCQ** as a function of different concentration of SO_3^{2-}. a) the fluorescence turn-on constants ($K_{\text{turn on}}$) was estimated to be 23.31 ± 6.23 μM (R^2 = 0.994); b) the detection limits for SO_3^{2-} was found to be 33 nM under the testing conditions.

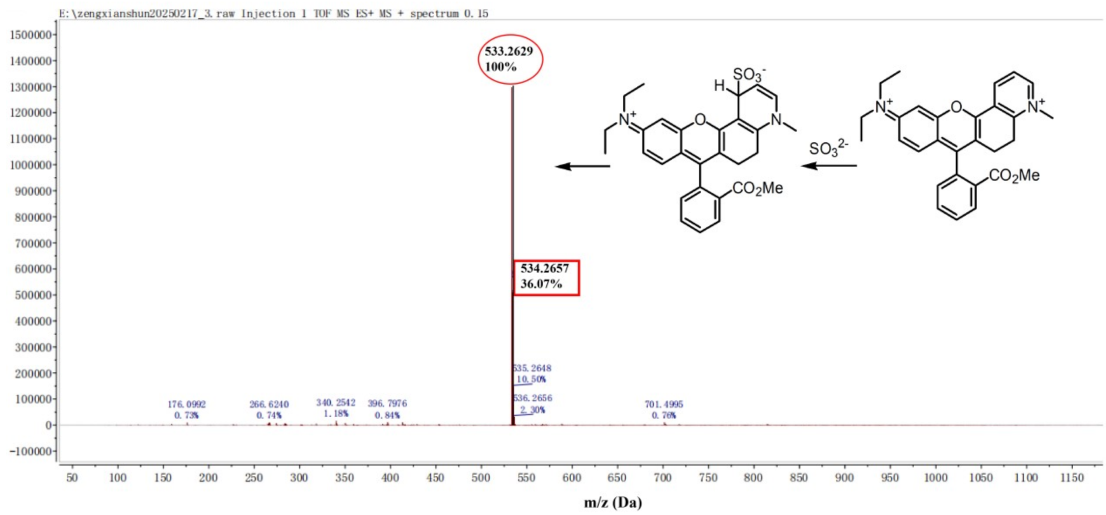

Fig. S9 HRMS spectrum of **DMCQ** in the presence of SO_3^{2-} in MeOH.

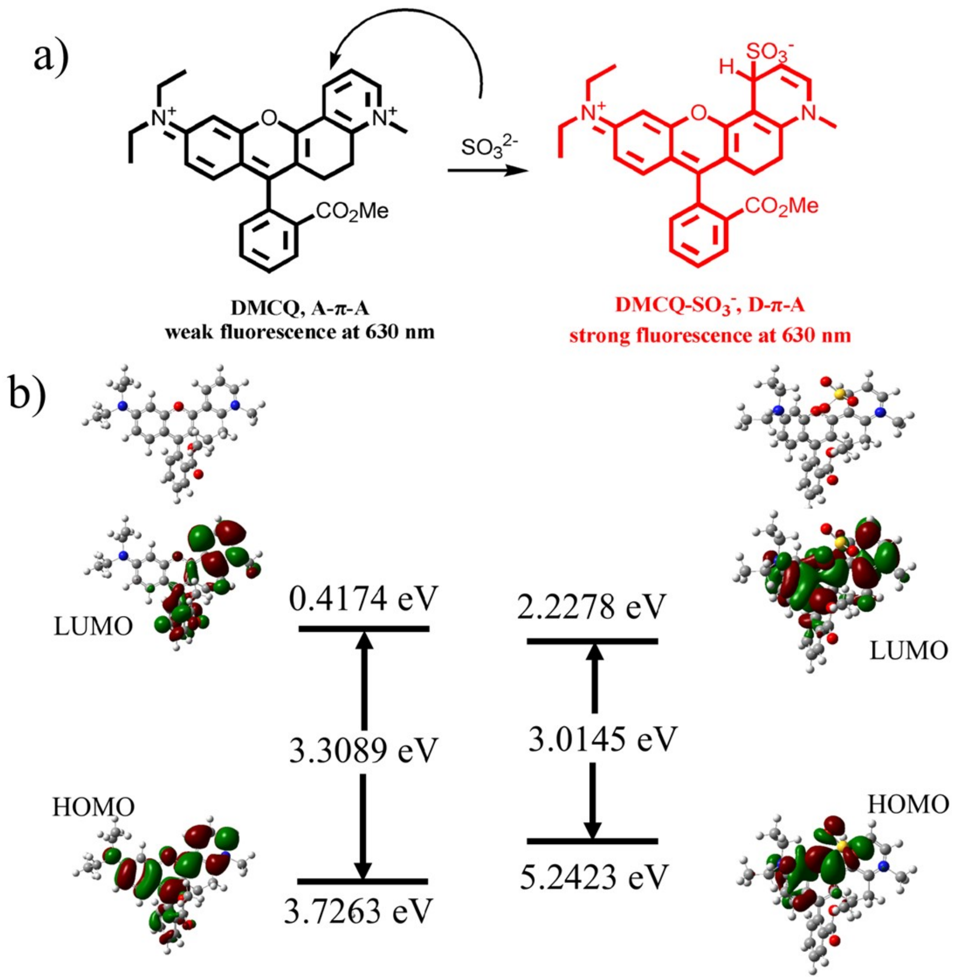

Fig. 10 Optimized structures, energy levels, and the molecular orbital plots of compounds **DMCQ** and **DMCQ-SO$_3^-$**.

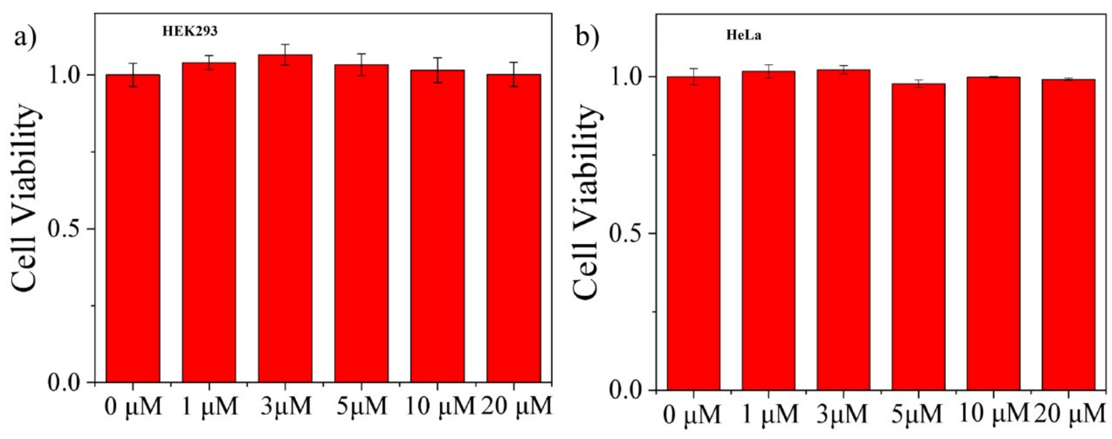

Fig. S11 Cytotoxicity of **DMCQ** in a) HEK293 cells and b) HeLa cells. The cells were incubated with **DMCQ** at corresponding concentrations (0 μM, 1 μM, 3 μM, 5 μM, 10 μM, 20 μM) for 24 h.

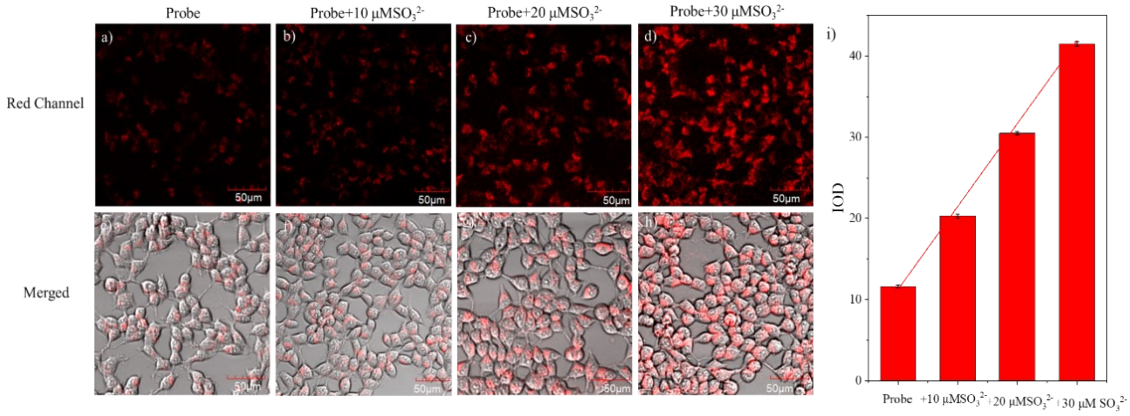

Fig. S12 (a-h) Fluorescence images of HEK293 cells incubated with **DMCQ** (3 μM) and varying concentrations of SO_3^{2-}. i) The corresponding average fluorescence intensity of the red channel. Incubation temperature: 37 °C; λ_{ex} = 559 nm, λ_{em} = 600-700 nm. Scale bar: 50 μm.

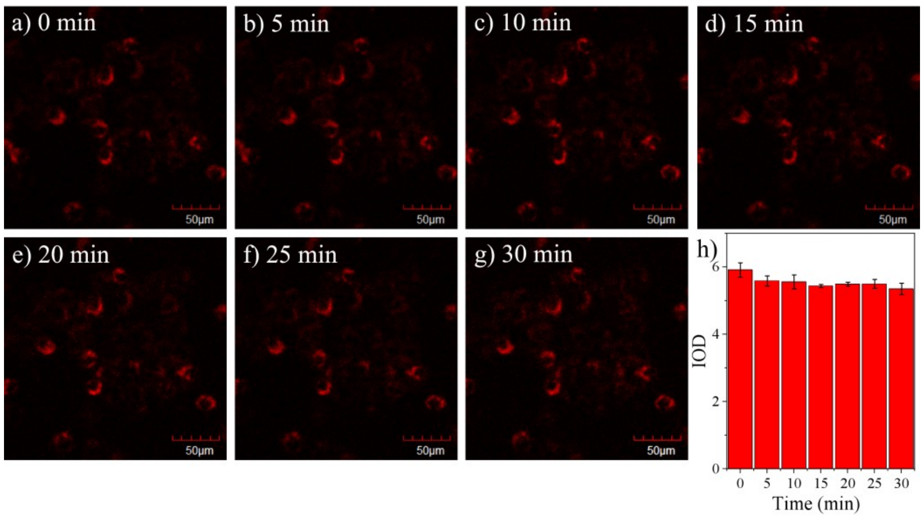

Fig. S13 Time-dependent confocal fluorescence imaging of the probe **DMCQ** in HeLa cells. (a-g) HeLa cells were incubated with the probe **DMCQ** (3 μM) for 30 min, then time-dependent imaging was carried out for 30 min, and the images were taken every 5 min for a total of 30 min; (h) The time-dependent fluorescence intensity changes of the probe **DMCQ** (3 μM) with continuous laser excitation. λ_{ex} = 559 nm, λ_{em} = 600-700 nm. Scale bar: 50 μm.

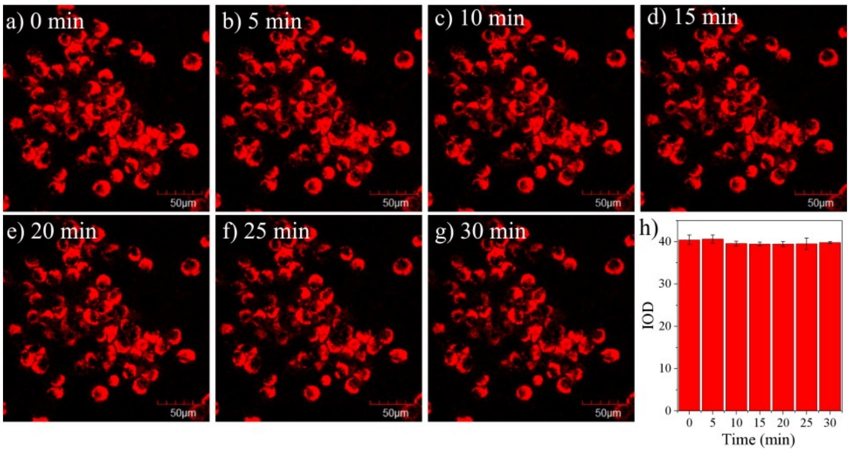

Fig. S14 Time-dependent confocal fluorescence imaging of the probe **DMCQ** after adding 20 equiv. SO_3^{2-} in HeLa cells. (a-g) HeLa cells were incubated with the probe **DMCQ** (3 μM) for 30 min, then adding 20 equiv. SO_3^{2-} for another 30 min; then time-dependent imaging was carried out for 30 min, and the images were taken every 5 min for a total of 30 min; (h) The time-dependent fluorescence intensity changes of the probe **DMCQ** (3 μM) with 20 equiv. SO_3^{2-} upon continuous laser excitation. λ_{ex} = 559 nm, λ_{em} = 600-700 nm. Scale bar: 50 μm.

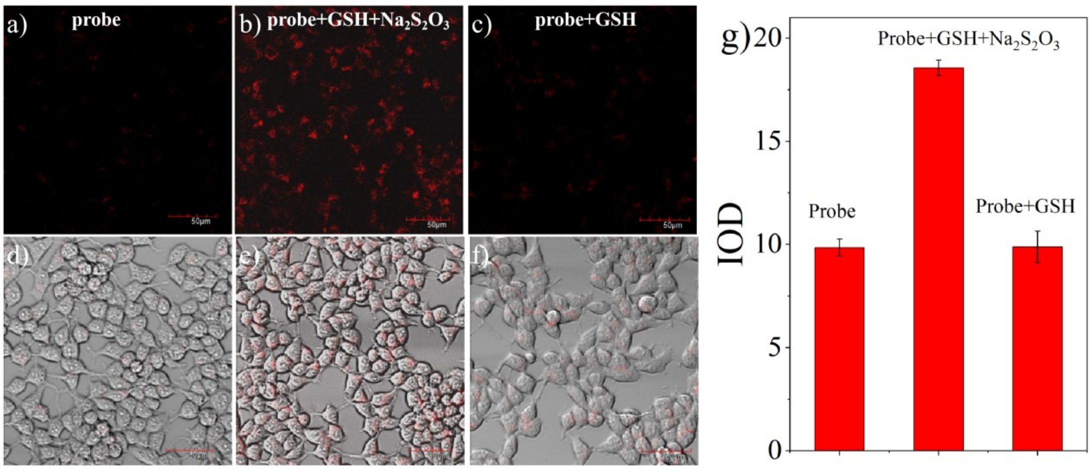

Fig. S15 Confocal images of HEK293 cells under different conditions: (a, d) incubating with **DMCQ** (3 μM); (b, e) incubating with GSH (600 μM) and $S_2O_3^{2-}$ (300 μM), then **DMCQ** (3 μM); (c, f) incubating GSH (600 μM), then **DMCQ** (30 μM); g) Average fluorescence intensity of the red channel. Incubation temperature: 37 °C; Incubation time: 30 min; λ_{ex} = 559 nm, λ_{em} = 600-700 nm. Scale bar: 50 μm.

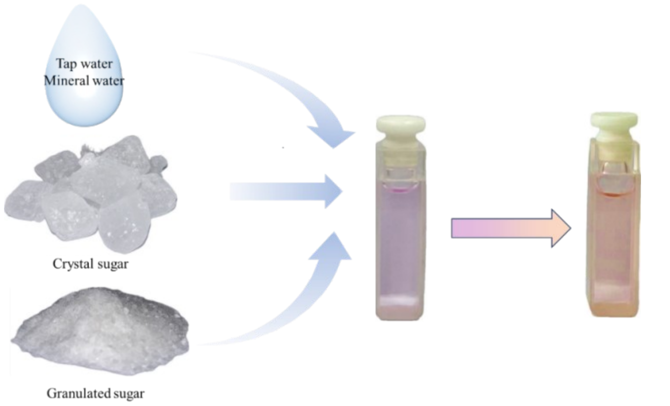

Fig. S16 Color of Granulated sugar, crystal sugar and water before and after the addition of SO_3^{2-}.

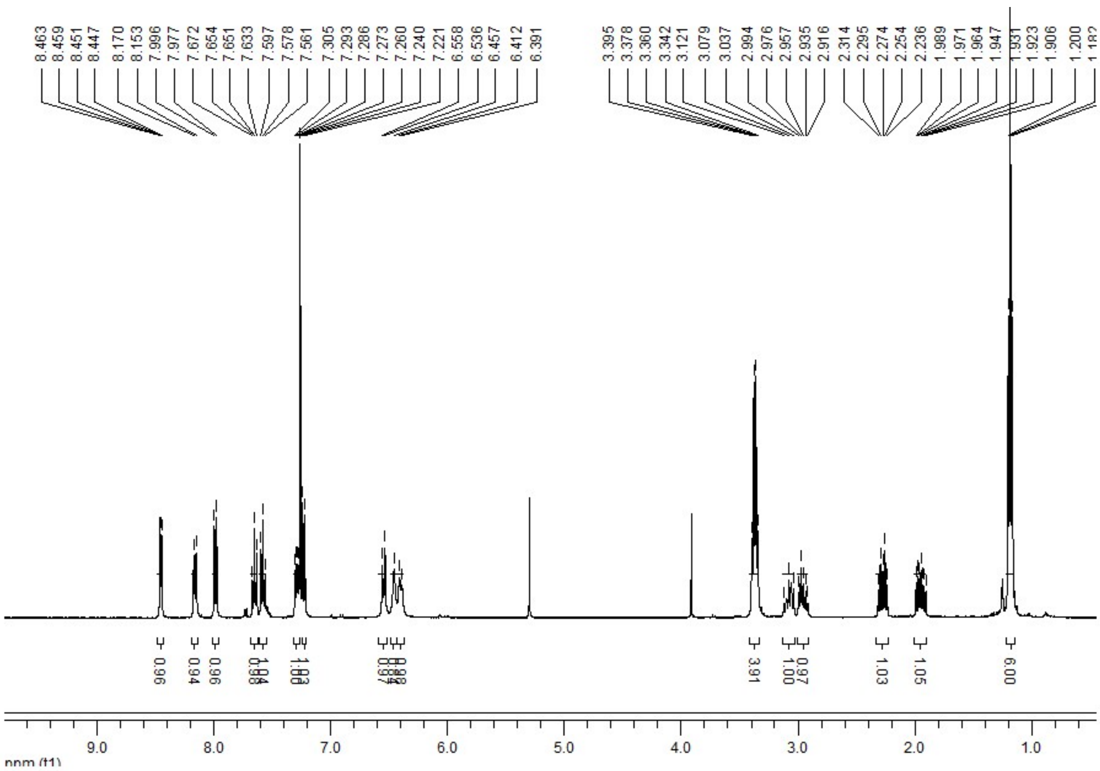

Fig. S17 ^{1}H NMR spectrum of the compound **1** (400 MHz, $CDCl_3$)

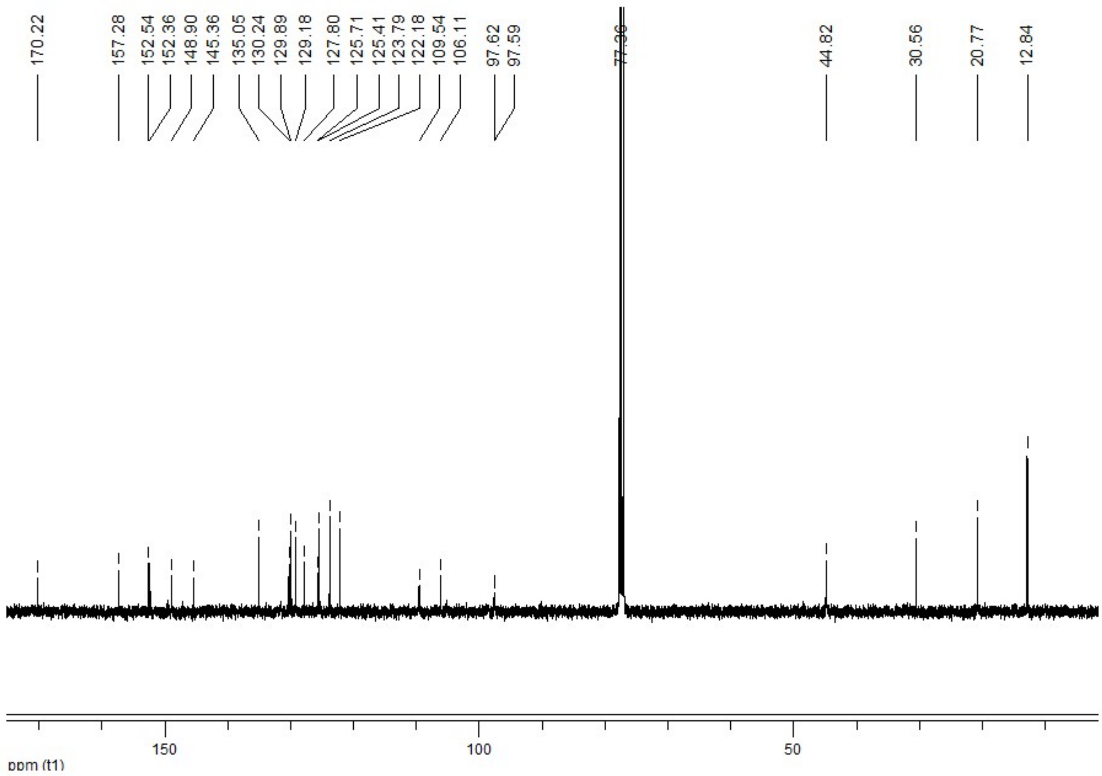

Fig. S18 ^{13}C NMR spectrum of the compound **1** (100 MHz, $CDCl_3$)

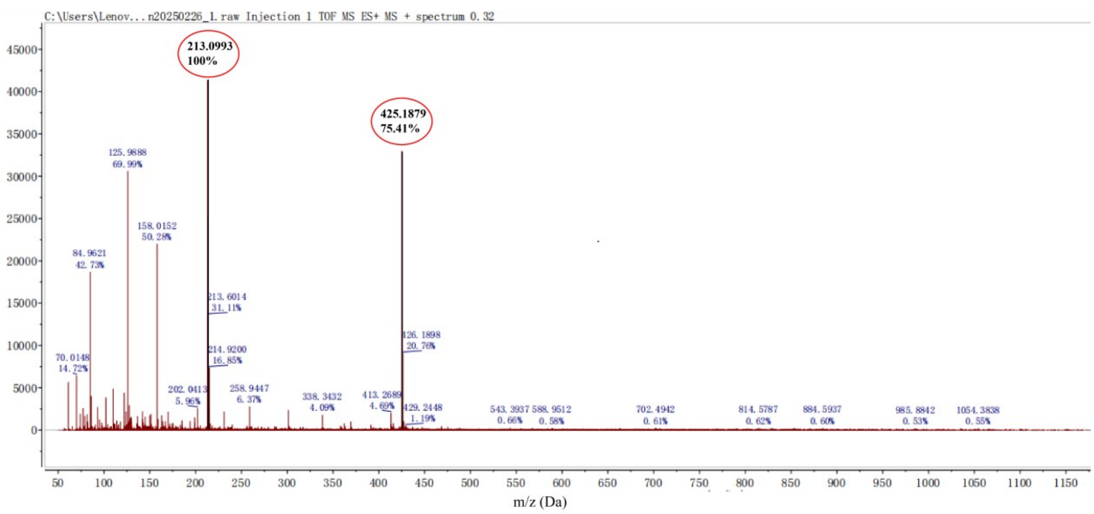

Fig. S19 HRMS spectrum of the compound **1**. The peak at m/z = 425.1879 was assigned to the mass of [**1+H**]$^+$, The peak at m/z = 213.0993 was assigned to the mass of [**M**/2+H]$^+$. **M** stands for compound **1**.

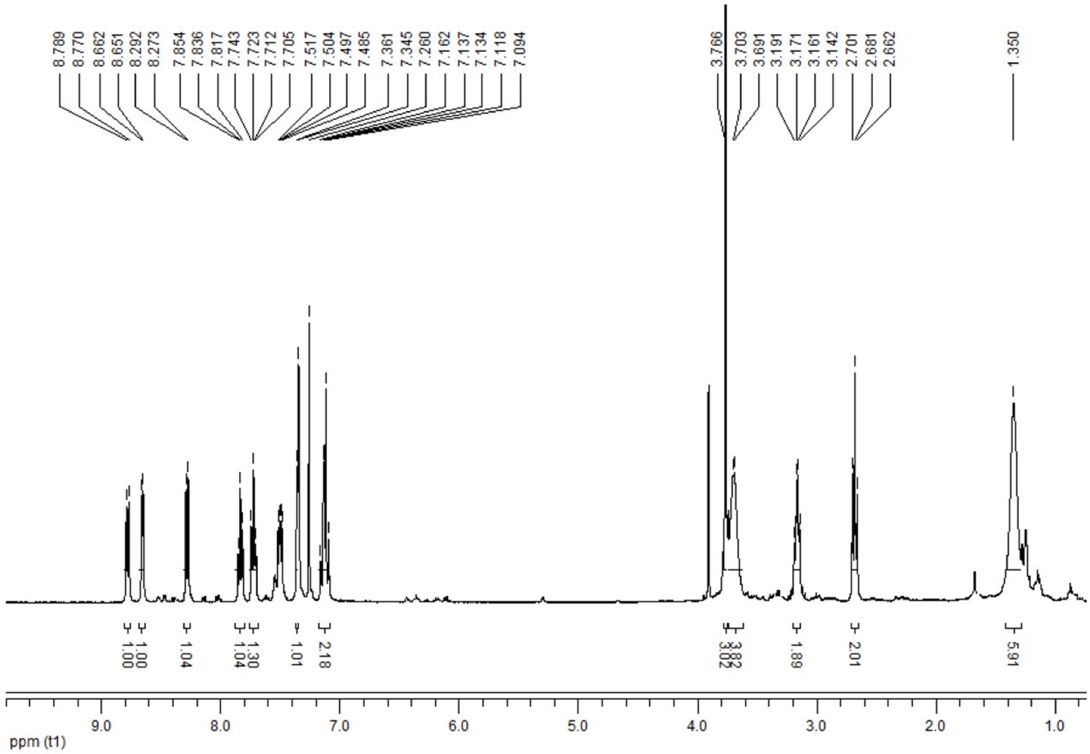

Fig. S20 ^{1}H NMR spectrum of the compound **2** (400 MHz, $CDCl_3$).

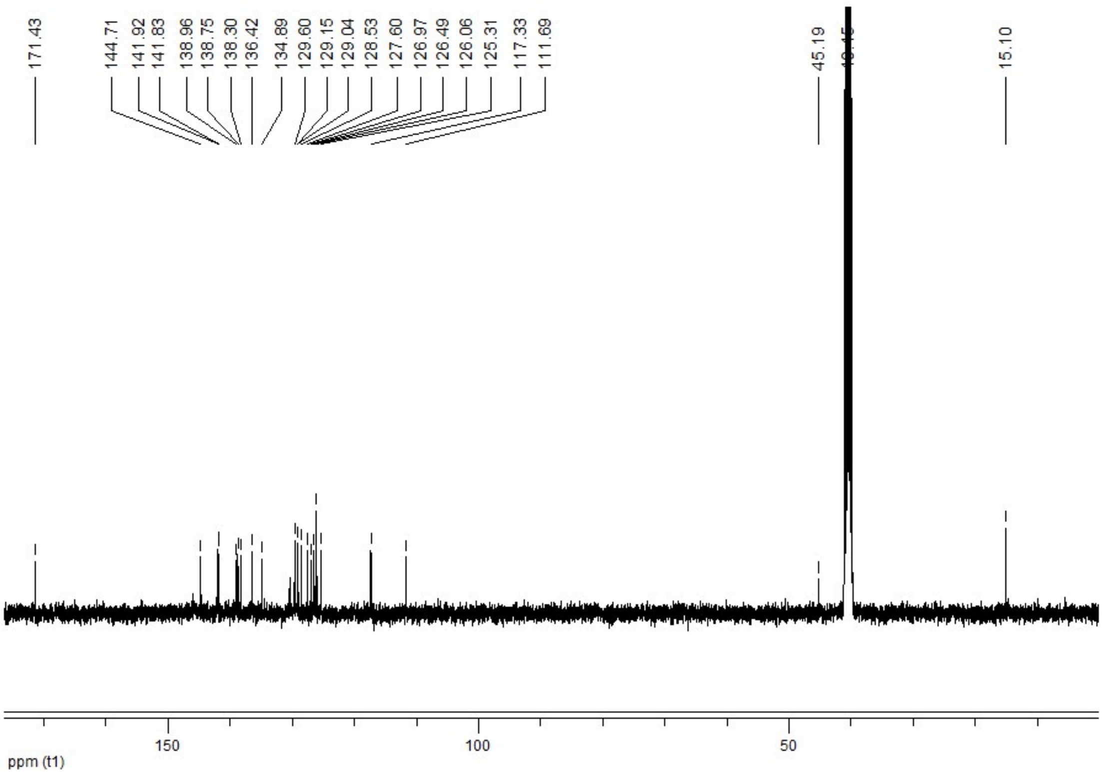

Fig. S21 ^{13}C NMR spectrum of the compound **2** (100 MHz, DMSO-d_6).

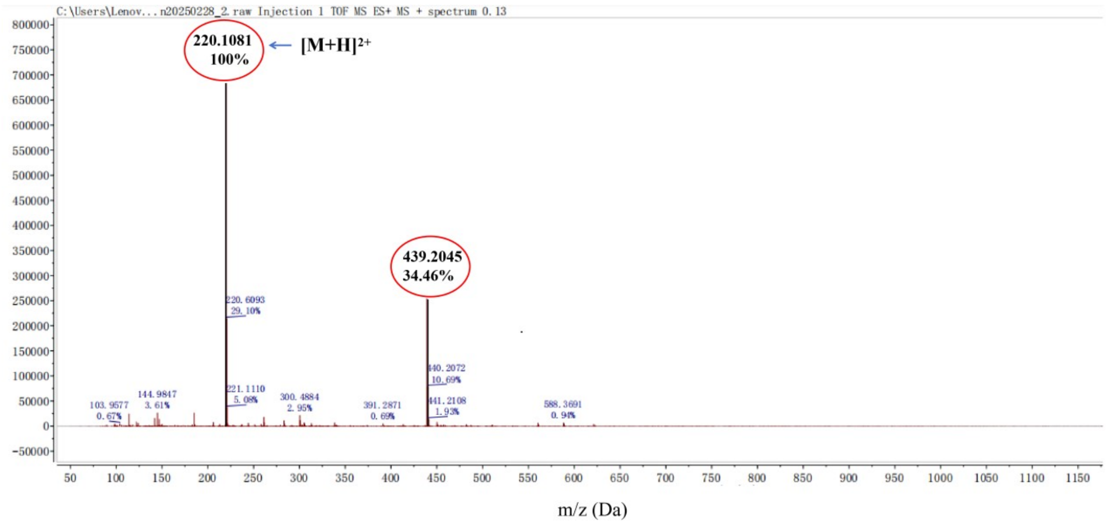

Fig. S22 HRMS (LC/MS) spectrum of the compound **2**. The peak at m/z = 439.2045 was assigned to the mass of [**2**]$^+$, the peak at m/z = 220.1081 was assigned to the mass of [**M**/2+H]$^+$. **M** stands for compound **2**.

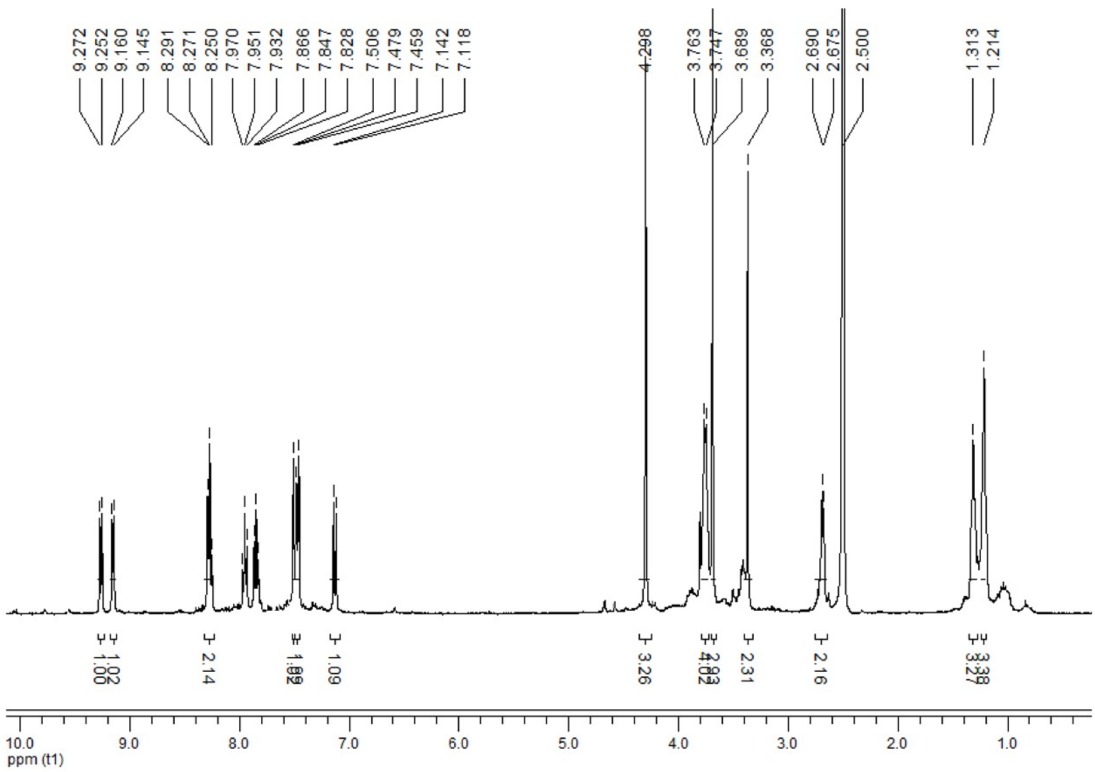

Fig. S23 ^{1}H NMR spectrum of the probe **DMCQ** (400 MHz, DMSO-d_6).

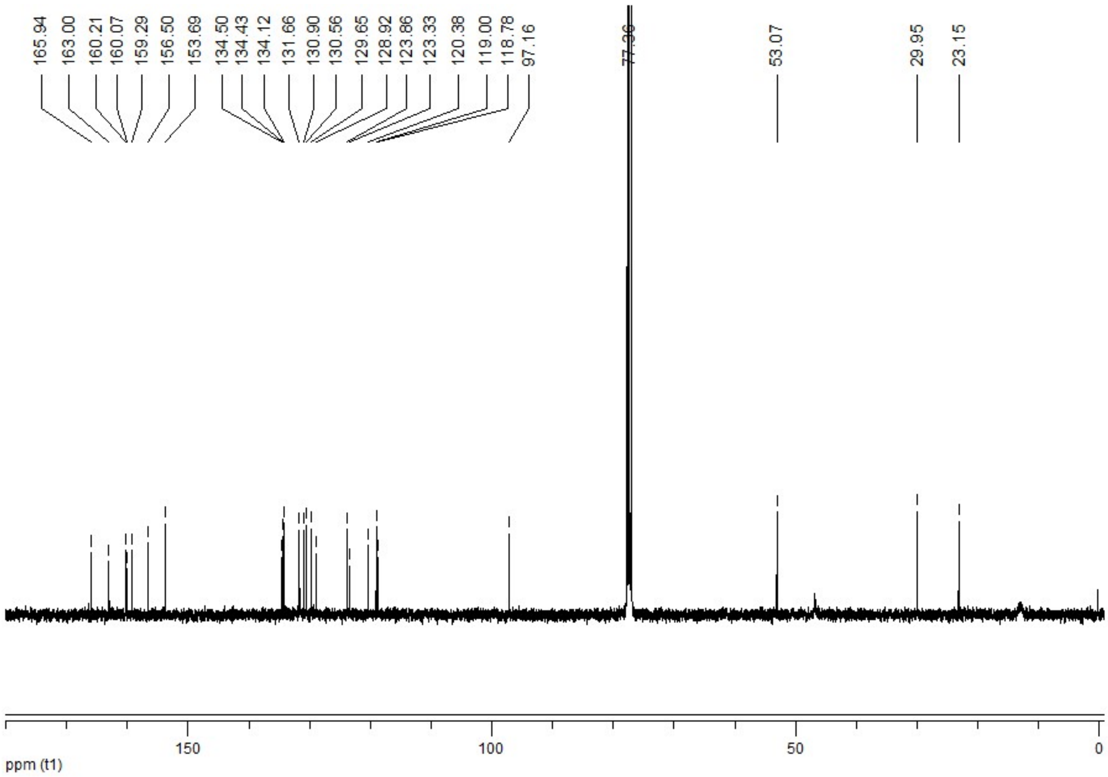

Fig. S24 ^{13}C NMR spectrum of **DMCQ** (100 MHz, $CDCl_3$).

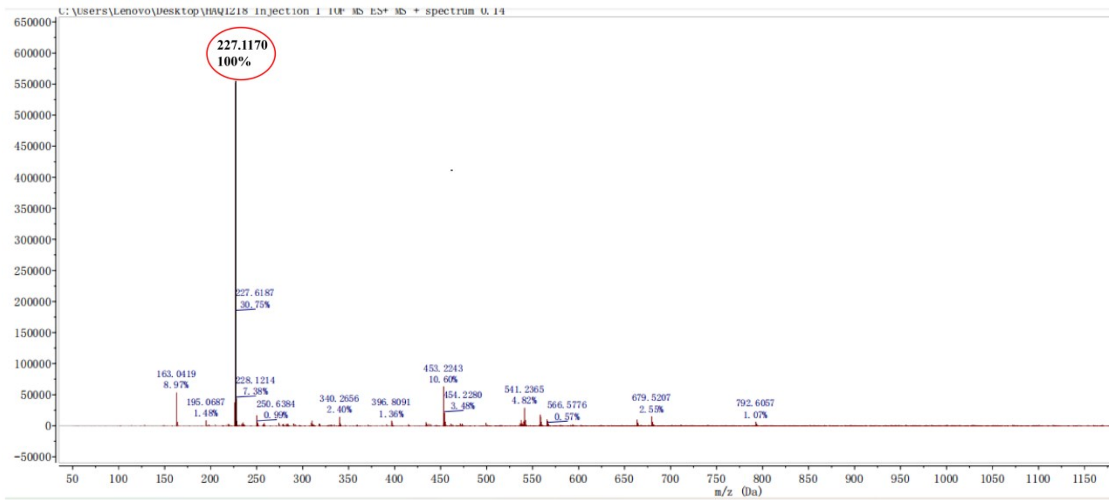

Fig. S25 HRMS spectrum of compound **DMCQ**. The peak at m/z = 227.1170 was assigned to the mass of [**DMCQ**/2]$^+$.

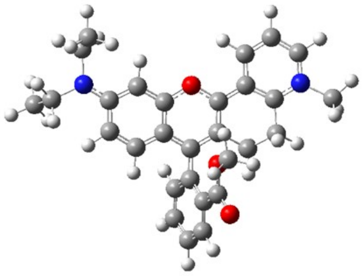

Fig. S26 Optimized structures and computed total energies of probe **DMCQ**.

Charge = 0 Multiplicity = 1

C	2.48719956	-1.32499296	-0.08905963
C	3.59663923	-0.56432878	-0.00246454
C	3.36949530	0.76110794	-0.05069485
C	2.13505659	1.26808756	-0.18996226
C	1.04607437	0.48404639	-0.30028138
C	1.23423299	-0.84563085	-0.22733641
C	-0.21140619	0.96104020	-0.44138572
C	-1.26777100	0.11404449	-0.50266229
C	-1.07524894	-1.21856978	-0.38838858
O	0.19319749	-1.72301245	-0.29294659
C	-2.65840619	0.60778565	-0.84846443
C	-3.73991783	-0.23564905	-0.18418507
C	-3.41985075	-1.69958331	-0.35577391
C	-2.12338065	-2.08154680	-0.41274125
N	-4.43174189	-2.54061730	-0.36673943
C	-4.13883673	-3.81188819	-0.44385287
C	-2.88817073	-4.28448084	-0.49207200
C	-1.87844821	-3.40627203	-0.46323305
C	-0.40821361	2.29113366	-0.58340634
C	-1.07630314	3.08620783	0.28994417
C	-1.26047020	4.38170493	-0.04457634
C	-0.78424893	4.89698498	-1.18744877

C	-0.09753236	4.11706528	-2.03000325
C	0.08214527	2.82606639	-1.72154691
N	4.80611896	-1.06801898	0.12886816
C	6.07249134	-0.22815846	0.31780504
C	6.68058474	0.16573806	-1.03333107
C	5.11451742	-2.56772333	0.10620882
C	5.01932122	-3.17260748	1.51161775
C	-5.89290477	-2.11594885	-0.26171175
C	-1.54445339	2.63021459	1.49835334
O	-2.15738940	3.36822755	2.24754907
O	-1.31486945	1.34458036	1.92928242
C	-1.63600973	0.99563583	3.25471688
H	2.55405866	-2.42264225	-0.03580538
H	4.18802609	1.49435135	0.01444706
H	2.05920392	2.36827218	-0.20011479
H	-2.85702260	1.67556659	-0.61815273
H	-2.75207270	0.51502162	-1.95823171
H	-3.77338380	-0.01830453	0.91026894
H	-4.71611502	0.06597573	-0.62642732
H	-4.96860992	-4.53787904	-0.45683599
H	-2.69589684	-5.36871793	-0.54789969
H	-0.85797574	-3.82211256	-0.49953194
H	-1.79558877	5.09261918	0.60682491
H	-0.94596233	5.96054347	-1.43196427
H	0.29838075	4.52910992	-2.97315811
H	0.61868864	2.19993413	-2.45707049
H	5.88351611	0.66720972	0.95023263
H	6.82392584	-0.80762811	0.90344531
H	7.60796358	0.76776033	-0.89441803
H	6.94606741	-0.73414567	-1.63325337

H	5.96830623	0.77481384	-1.63463359
H	4.46041303	-3.11225377	-0.61027242
H	6.14059539	-2.73450771	-0.29741184
H	5.25306919	-4.26196139	1.49492802
H	5.73413906	-2.68222254	2.21076344
H	3.99636211	-3.05217811	1.93459577
H	-6.05081021	-1.44915164	0.61603931
H	-6.21502333	-1.60350946	-1.19652640
H	-6.57377227	-2.98388965	-0.11557464
H	-1.30339222	-0.05399239	3.41784745
H	-1.09492569	1.65533574	3.96918824
H	-2.73742113	1.04377492	3.40834118

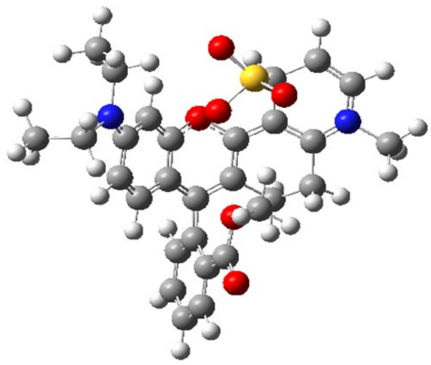

Fig. S27 Optimized structures and computed total energies of probe **DMCQ-SO_3^-**.

M062X/DEF2TZVP

Charge = 0 Multiplicity = 1

C	-2.17245000	-0.19963800	-1.09682200
C	-2.87606800	-1.05647600	-0.34336900
C	-2.25318300	-2.21938600	-0.06556200
C	-0.97092800	-2.44972400	-0.39877300
C	-0.21977400	-1.47436000	-0.94008100
C	-0.86489600	-0.36491500	-1.33679100
C	1.13117300	-1.50103600	-1.05019600
C	1.78232600	-0.31321400	-1.13354900

C	1.04794900	0.79754400	-1.33796200
O	-0.17448300	0.64232200	-1.91543000
C	3.25203900	-0.14516000	-0.85404400
C	3.46856700	1.01862600	0.10720300
C	2.59131800	2.21965100	-0.20115300
C	1.42613900	2.00481400	-0.85793900
N	2.87308400	3.41463300	0.16664200
C	2.21646200	4.48732800	-0.02293800
C	1.02246000	4.44905300	-0.62043800
C	0.39762200	3.12726400	-0.95142000
C	1.83005700	-2.59066000	-0.67445900
C	2.04317500	-3.00328600	0.59958600
C	2.72831000	-4.15441800	0.77357900
C	3.20566600	-4.86425000	-0.26000800
C	3.01178200	-4.43222200	-1.51167800
C	2.32557800	-3.29893300	-1.70848900
N	-4.08474200	-0.72813400	0.05482100
C	4.15994500	3.61057800	0.90369600
C	-4.92684500	-1.68252200	0.90809200
C	-4.80623600	0.55562700	-0.38062800
C	-6.19980400	0.87582000	0.18008700
C	-5.71635500	-2.66155800	0.03099400
C	1.60430800	-2.30027100	1.69605400
O	1.81501600	-2.72361200	2.81733300
O	0.95690900	-1.09660900	1.57580500
C	0.73736400	-0.31413900	2.72424200
S	-0.93471800	2.90687200	0.21325900
O	-2.27187800	3.08288000	-0.35476200
O	-0.59190800	3.11483700	1.62118300
O	-1.51358900	1.41302900	0.70767100

H	-2.60095800	0.74670300	-1.45820400
H	-2.75414600	-3.02758300	0.48865400
H	-0.52547400	-3.40817300	-0.08453100
H	3.75325800	-1.05549700	-0.45620100
H	3.73541600	0.08014500	-1.83528700
H	3.22200700	0.69170400	1.14601800
H	4.55565700	1.26026300	0.07396100
H	2.62881200	5.45216300	0.30761700
H	0.44783100	5.37593400	-0.78606500
H	-0.00774600	3.19935600	-1.98756900
H	2.94522800	-4.57093000	1.77130100
H	3.76602500	-5.79817100	-0.08411100
H	3.40466400	-5.00597500	-2.36742000
H	2.16269700	-2.96625100	-2.74919200
H	4.25841400	2.89444400	1.75091400
H	5.02693100	3.50840300	0.21104400
H	4.26218500	4.60784400	1.38663900
H	-4.30105000	-2.23348500	1.64431000
H	-5.61832400	-1.11918000	1.57045700
H	-4.17717800	1.42762500	-0.08714600
H	-4.90219700	0.53825200	-1.49386200
H	-6.58827000	1.82616000	-0.25501000
H	-6.94453300	0.08757300	-0.06941500
H	-6.18004100	1.02145700	1.28413300
H	-6.34656700	-3.33784500	0.65305100
H	-6.38802300	-2.12510100	-0.67601900
H	-5.03453700	-3.29855700	-0.57659400
H	0.36639100	0.67957900	2.39319600
H	-0.03447500	-0.79167400	3.36813800
H	1.69037000	-0.15823900	3.27700700

[S1] T. Karstens, K. Kobs, Rhodamine B and Rhodamine 101 as reference substances for fluorescence quantum yield measurements. *J. Phys. Chem.*, 1980, 84, 1871-1872.

[S2] F. Ma, M. Liu, Z. Wang, C. Zhang, Multiplex detection of histone-modifying enzymes by total internal reflection fluorescence-based single-molecule detection, *Chem. Commun.*, 2016, 52, 1218-1221.

[S3] P. Du, S, J. Lippard, A highly selective turn-on colorimetric, red fluorescent sensor for detecting mobile zinc in living cells, *Inorg. Chem.,* 2010, 49, 10753-10755.